1521-009X/48/8/698–707$35.00
DRUG METABOLISM AND DISPOSITION

https://doi.org/10.1124/dmd.120.000009
Drug Metab Dispos 48:698–707, August 2020

Excretion, Mass Balance, and Metabolism of [^{14}C]LY3202626 in Humans: An Interplay of Microbial Reduction, Reabsorption, and Aldehyde Oxidase Oxidation That Leads to an Extended Excretion Profile

Kishore Katyayan, Ping Yi,[1] Scott Monk, and Kenneth Cassidy

Drug Disposition Eli Lilly and Company, Indianapolis, Indiana

Received March 12, 2020; accepted April 22, 2020

ABSTRACT

The mass balance, excretion, and metabolism of LY3202626 were determined in healthy subjects after oral administration of a single dose of 10 mg of (approximately 100 μCi) [^{14}C]LY3202626. Excretion of radioactivity was slow and incomplete, with approximately 75% of the dose recovered after 504 hours of sample collection. The mean total recovery of the radioactive dose was 31% and 44% in the feces and urine, respectively. Because of low plasma total radioactivity, plasma metabolite profiling was conducted by accelerator mass spectrometry. Metabolism of LY3202626 occurred primarily via *O*-demethylation (M2) and amide hydrolysis (M1, M3, M4, and M5). Overall, parent drug, M1, M2, and M4 were the largest circulating components in plasma, and M2 and M4 were the predominant excretory metabolites. The slow elimination of total radioactivity was proposed to result from an unusual enterohepatic recirculation pathway involving microbial reduction of metabolite M2 to M16 in the gut and reabsorption of M16, followed by hepatic oxidation of M16 back to M2. Supporting in vitro experiments showed that M2 is reduced to M16 anaerobically in fecal homogenate and that M16 is oxidized in the liver by aldehyde oxidase to M2. LY3202626 also showed a potential to form a reactive sulfenic acid intermediate. A portion of plasma radioactivity was unextractable and presumably bound covalently to plasma proteins. In vitro incubation of LY3202626 in human liver microsomes in the presence of NADPH with dimedone as a trapping agent implicated the formation of the proposed sulfenic acid intermediate.

SIGNIFICANCE STATEMENT

The excretion of radioactivity in humans after oral administration of a single dose of 10 mg of [^{14}C]LY3202626 was very slow. The results from in vitro experiments suggested that an interplay between microbial reduction, reabsorption, and aldehyde oxidase oxidation (M2 → M16 → M2) could be a reason for extended radioactivity excretion profile. In vitro metabolism also showed that LY3202626 has the potential to form a reactive sulfenic acid intermediate that could potentially covalently bind to plasma protein and result in the observed unextractable radioactivity from plasma.

Introduction

Alzheimer disease is an incurable neurodegenerative disease characterized by a progressive deterioration of cognition and function and is the most common cause of dementia. Accumulation of protein in the brain, specifically extracellular plaques comprising the β-amyloid peptide and intracellular neurofibrillary tangles of hyperphosphorylated τ, is believed to be linked to neuronal losses in specific brain regions, giving rise to losses in memory, learning, and cognition. The β-site amyloid precursor protein-cleaving enzyme 1 (BACE1) plays a critical role in the production of β-amyloid peptides, and consequently, BACE1 inhibitors have been aggressively investigated as potential Alzheimer therapies. LY3202626, a synthetic small molecule and a potent BACE1 inhibitor, was recently evaluated as a potential treatment of early Alzheimer disease.

Determination of excretion, mass balance, and metabolism of a drug candidate in humans after a dose of radiolabeled drug is one of the most critical steps in drug development (Roffey et al., 2007; Penner et al., 2009). Although in vitro and preclinical studies (including ^{14}C preclinical studies) may be helpful in designing early clinical studies, the radioactive clinical study provides the most definite information regarding primary mechanism(s) of clearance, along with the quantitative and comprehensive metabolite profiles in human plasma and excreta. Defining the routes of clearance is crucial for understanding potential interindividual variability as well as for planning appropriate clinical pharmacology studies, such as drug-drug interaction studies and studies in special populations (renally and hepatically impaired subjects, for example). Characterization of metabolites in this study is important in determining which, if any, metabolites meet regulatory criteria

This work was supported by Eli Lilly and Company.
[1]Current affiliation: Covance, Madison, Wisconsin.
The work was presented at International Society for the Study of Xenobiotics, Portland OR, 2019 as a poster.
https://doi.org/10.1124/dmd.120.000009.
This article has supplemental material available at dmd.aspetjournals.org.

ABBREVIATIONS: A, apical; ABT, 1-aminobenzotriazole; AMS, accelerator mass spectrometry; AO, aldehyde oxidase; AUC, area under the concentration versus time curve; B, basolateral; BACE1, β-site amyloid precursor protein-cleaving enzyme 1; HPLC High Performance Liquid Chromatography LC-MS, liquid chromatography mass spectrometry; LC Liquid Chromatography LC-MS/MS, liquid chromatography tandem mass spectrometry; LSC, liquid scintillation counting; MDCK, Madin-Darby Canine Kidney; MDR1, Multidrug Resistance Protein 1; P-gp, P-glycoprotein; PK, Pharmacokinetics; t_{max}, time of maximum observed drug concentration.

(i.e., metabolites accounting for ≥10% of the total circulating drug–related exposure) requiring testing in toxicology studies and evaluation of DDI potential(FDA, 2020a) (FDA, 2020b)(FDA, 2020a,b). The present clinical study was conducted to determine the disposition of radioactivity and LY3202626 in healthy male subjects after oral administration of a pharmacological dose of LY3202626 containing [^{14}C]LY3202626. The total administered dose was 10 mg, which was supported by the available safety data. Data from previous clinical studies indicated that a 10-mg dose was safe and well tolerated and would result in substantial reductions of plasma and cerebrospinal fluid amyloid β, suggesting a dose in this range would likely be used in subsequent clinical efficacy studies. The radiotracer was administered at approximately 100 μCi to each subject to facilitate characterization of the physiologic disposition and metabolism of LY3202626. The quantitative whole-body autoradiography disposition study for LY3202626 in male rats and dosimetry calculations showed that the administration of a single 100-μCi oral dose of [^{14}C]LY3202626 would not be expected to represent a significant radiation exposure risk to healthy human subjects. Results from this study led us to conduct several in vitro metabolism experiments to better understand the disposition and clearance pathways of LY3202626 in humans.

Materials and Methods

LY3202626, [^{14}C]LY3202626, LSN3200635 (M1), LSN3207841 (M2), LSN3329581 (M4), LSN3226305 (M5), and LSN3420637 (M16) were synthesized by Eli Lilly and Company. For clinical trial use, the investigational drug was supplied as powder in a bottle and was administered as an oral solution in degassed Sprite Zero. Rat (pooled male Sprague-Dawley, $n = 10$), dog (pooled male beagle, $n = 3$), monkey (pooled male cynomolgus, $n = 3$), and human hepatocytes (pooled mixed sex, $n = 50$) and fecal homogenates (pooled male, $n = 3$) were obtained from Bioreclamation/IVT (Westbury, NY), whereas human liver cytosol (mixed sex, $n = 100$) was obtained from Xenotech (Lenexa, KS). All other reagents or materials used herein were purchased from Sigma-Aldrich (St. Louis, MO), excluding all cell culture products, which were from Invitrogen Life Technologies (Carlsbad, CA), unless otherwise stated.

Clinical Study Design and Sample Collection. The study was conducted at Covance Clinical Research Unit Inc. in Madison WI in six healthy male subjects between the ages of 27 and 58 years old (one Asian, two African Americans, and three Caucasians). The study was conducted in compliance with ethical principles that have their origin in the Declaration of Helsinki and was approved by the institutional review boards at MidLands Independent Review Board (Tampa, FL) and Covance Clinical Research Unit Inc. After fasting overnight, each of the six subjects received a single 10-mg oral dose of LY3202626 containing approximately 100 μCi of [^{14}C]-LY3202626 as an oral solution. Subjects continued to fast up to 4 hours postdose. Whole blood and plasma samples were collected at the following time points: 0 (predose), 0.5, 1, 2, 3, 4, 5, 6, 8, 10, 12, 24, 36, 48, 72, 96, 120, 144, and 168 hours postdose, and every 24 hours thereafter until the study discharge criteria had been met. Additional venous blood samples (approximately 15 ml each) were drawn for metabolite profiling predose and at 1, 2, 4, 8, 24, and 48 hours postdose.

Urine samples were collected over the following intervals: before study drug administration (predose); 0–6, 6–12, 12–24, 24–48, and 48–72 hours postdose; and at 24-hour intervals thereafter until the study discharge criteria had been met. Feces were collected predose and at 24-hour intervals until discharge criteria were met and then mixed with a weighed amount of acetonitrile:water (1:1, v:v) and homogenized. Samples were stored at −20°C until analysis. Samples of expired air were collected for the analysis of $^{14}CO_2$ prior to dosing on day 1 (negative control sample) and at 2, 4, 8, and 24 hours postdose. Subjects remained at the Clinical Research Unit for up to a maximum of 21 days postdose and were discharged from the Clinical Research Unit at any time after 24-hour urine and fecal samples from two consecutive collections each had radioactivity levels less than 1.0% of the total administered radioactivity in urine and feces combined or day 22 (21 days postdose). This study was registered at clinicaltrials.gov with the identifier NCT02555449.

Analysis of Total Radioactivity and LY3202626. Radioactivity in blood, plasma, urine, and feces was measured by liquid scintillation counting (LSC) either directly (in urine, plasma, and expired air) or after combustion in an oxidizer apparatus followed by liquid scintillation counting of the trapped $^{14}CO_2$ at Covance Laboratories. LY3202626 concentrations in plasma were determined with a validated LC-MS/MS assay at Covance Bioanalytical Services, LLC (Indianapolis, IN), using positive ion TurboIon Spray on a Sciex API 3000 mass spectrometer. Details of the assays can be found in Supplemental Materials and Methods.

Metabolite Profiling of Plasma, Urine, and Feces. A single plasma AUC pool (Hamilton et al., 1981; Hop et al., 1998) was generated from 0 to 24 hours after pooling individual time points across subjects [0 (predose), 1, 2, 4, 8, and 24 hours]. Individual time points of plasma samples at 4, 48, 144, 288, and 504 hours were also pooled across subjects. The AUC pool and the pooled 4-, 144-, and 288-hour samples were profiled by high performance liquid chromatography (HPLC) fraction collection with UV in line and then off-line accelerator mass spectrometry (AMS) (Xceleron, Germantown, MD). The pooled 48- and 504-hour plasma samples were not profiled by HPLC and only "counted" for total radioactivity by AMS. For extraction, initially a protein precipitation procedure was employed. However, because of the poor extraction recovery, the plasma samples were diluted 5- or 10-fold and injected directly onto the HPLC system and fractionated for AMS analysis. Radiochromatograms from the AMS results were generated, and LY3202626 and metabolites were expressed as the percentage of region of interest, with the sum of all integrated peaks defined as 100%. Details of the analysis of plasma are shown in Supplemental Materials and Methods.

Metabolite profiling and identification of metabolites in human urine and feces were performed by Eli Lilly and Company. Metabolites in the urine and feces were profiled by high-performance liquid chromatography fraction collection with off-line radioactivity counting, and metabolites were identified using LC-MS. Three pooled urine samples (0–24, 24–312, and 480–504 hours) were prepared by pooling the same percentage of urine sample from each collection for individual subjects and then pooling across subjects. The pooled urine samples were extracted using Agilent Bond Elut Plexa PCX cartridges (60 mg, 3 ml). Four pooled feces samples (0–24, 24–96, 96–336, and 480–504 hours) were prepared by pooling the same percentage of homogenized feces sample from each collection for individual subjects and then pooling across subjects. Pooled fecal samples were extracted first with methanol/acetonitrile (50/50) followed by Agilent Bond Elut Plexa PCX extraction for further cleanup. The urine and feces samples were analyzed using radio/HPLC and mass spectrometry. Detailed extraction and analysis methods are provided in the Supplemental Materials and Methods.

LSN3420637 (M16) In Vitro Hepatocyte Incubations. LSN3420637 (M16) was incubated with rat, dog, monkey, and human hepatocytes in suspension at 1 million cells per milliliter with a substrate concentration 10 μM with or without 1-aminobenzotriazole (ABT) (1 mM) or hydralazine (200 μM) at 37°C for 4 hours. An equal volume of acetonitrile was added to quench the reaction at the end of incubation. The samples were centrifuged, and the supernatants were analyzed by a ultra high performance liquid chromatography system using a waters Acquity BEH C18, 2.1 × 10 cm (1.7-μm particle size), and following the liquid chromatography (LC) condition: mobile phase A (water containing 0.2% formic acid); mobile phase B (acetonitrile); flow rate = 0.5 ml/min; and gradient (min/B %) = 0/5, 0.4/5, 3.5/50, 5/90, 6/90, 6.1/5, 8/stop. Accurate mass LC-MS and LC-MS/MS [Thermo OrbiTrap Velos mass spectrometer fitted with heated electrospray ionization (Thermo Fisher Scientific) with positive ion detection] were used for parent and metabolite identification [spray voltage = 4.5 kV, capillary temperature = 300°C, source heater temperature = 350°C, sheath gas = 60, auxiliary gas = 20, sweep gas = 20, higher-energy collisional dissociation = 35].

LSN3420637 (M16) Incubation in Human Liver Cytosol and M2 Isolation. LSN3420637 was incubated with human liver cytosol at 1 mg/ml protein with substrate concentration 50 μM at 37°C for 4 hours. The total volume of incubation was approximately 80 ml. An equal volume of acetonitrile was added to quench the reaction at the end of incubation. The samples were centrifuged, and the supernatant was concentrated to approximately 20 ml in GeneVac (a vacuum centrifugal evaporator) for M2 isolation.

M2 isolation was conducted by a semipreparative HPLC system using a C18 HPLC column (25 × 10 mm; 5-μm particle size) and following the LC condition: mobile phase A (0.2% formic acid); mobile phase B [acetonitrile/methanol

(25/75)]; flow rate = 6 ml/min, and gradient (minutes/B%) = 0/20, 5/20, 20/50, 21/90, 30/90, 30.1/20, 55/stop. Fractions were collected at 15-second intervals. Selected fractions were analyzed by LC-MS. Fractions containing high purity of M2 were combined, freeze-dried, and submitted for NMR analysis.

LSN3207841 (M2) Incubation with Human Fecal Microflora. The fecal homogenates were purchased from Bioreclamation Inc. (New York). Fresh feces were collected from three healthy subjects individually. Upon collection, feces were mixed with 10% glycerol in 100 mM sodium phosphate buffer (pH 7.4) (1:4, w:v) and homogenized. The homogenates were stored at −70°C until use. Fecal homogenates pooled from the three subjects were used for this experiment. To deactivate fecal bacteria, an aliquot of fecal homogenate was placed in a 100°C water bath for 1 hour. The heated and nonheated fecal homogenates were inoculated in brain heart infusion medium (Remel Inc.) containing 10 μM test compound and incubated under anaerobic atmosphere for 1 week in a desiccator at 37°C. The anaerobic atmosphere in the desiccator was created by placing two AnaeroGen paper sachets (Oxoid, Ld.) into the desiccator. An anaerobic indicator pill was also placed in the desiccator to monitor anaerobic status. After 1 week of incubation, samples were extracted with acetonitrile and analyzed by LC-MS as described above.

NMR Identification of M2 from In Vitro Incubation of M16. NMR identification of M2 was performed on Bruker 600 AVANCE III HD (Bruker BioSpin Corporation, San Jose, CA) instruments with field strengths of 14.1 T with CP QCI 600S3 H/F-C/N-D-05 Z probe. All analytes were dissolved in CD_3OD, and the experiments were conducted at 25°C. Standard proton spectra were used to confirm the structure of the metabolite. Spectra were referenced with respect to water signal at 3.31 ppm for ^1H.

LY3202626 Incubation with Human Liver Microsomes and Dimedone. LY3202626 (1 μM) was incubated with human liver microsomes at 1 mg/ml, 2 mM dimedone, and 2 mM NADPH in a total volume of 1 ml (100 mM phosphate buffer, pH 7.4) for 45 minutes at 37°C in a shaking water bath. The reaction was stopped by 2 ml of acetonitrile and then centrifuged for approximately 10 minutes at 4000 rpm, and samples were analyzed by an HPLC system using a Waters Acquity BEH C18, 2.1 × 100 mm (1.7-μm particle size), and following the LC condition: mobile phase A (water containing 0.2% formic acid); mobile phase B (acetonitrile); flow rate = 0.5 ml/min; and gradient (minutes/B%) = 0/5, 0.4/5, 3.5/50, 4/90, 4.25/90, 4.5/5, 6/stop. Accurate mass LC-MS and LC-MS/MS (Waters Synapt G2-S) were used for parent compound and dimedone adduct identification (electrospray ionization positive, capillary = 1.0 kV, sample cone = 40 V, source temperature = 120°C, desolvation = 500°C, and collision energy = 10–35 V).

In Vitro Assessment of Permeability of LSN3420637 (M16) and LSN3207841 (M2). Madin-Darby Canine Kidney (MDCK) cells transfected with Multidrug Resistance Protein 1 (MDR1) ATP binding cassette subfamily B member 1 (ABCB1) obtained at passage number 12 from P. Borst at The Netherlands Cancer Institute (Amsterdam, The Netherlands) were used for apical-to-basolateral (A-B) and basolateral-to-apical (B-A) flux determination of LSN3420637 (M16) and LSN3207841 (M2). Details of the method and analysis are provided in the Supplemental Materials and Methods.

Pharmacokinetic Analysis. Pharmacokinetic parameter estimates of total radioactivity (in blood and plasma) and LY3202626 (in plasma) were calculated by standard noncompartmental methods of analysis using Phoenix WinNonlin version 6.2.1. The primary pharmacokinetics (PK) parameters calculated included maximum observed drug concentration (C_{max}); time of maximum observed drug concentration (t_{max}); area under the concentration versus time curve (AUC) from time zero to time t, where t was the last time point with a measurable concentration [$AUC_{(0–tlast)}$]; AUC from zero to infinity [$AUC_{(0–\infty)}$]; percentage of $AUC_{(0–\infty)}$ extrapolated [$\%AUC_{(tlast–\infty)}$]; and half-life associated with the terminal rate constant in noncompartmental analysis ($t_{1/2}$). For LY3202626 in plasma, additional non-compartmental parameters, including apparent total body clearance of drug after extravascular administration (CL/F), apparent volume of distribution during the terminal phase after extravascular administration (V_z/F), and apparent volume of distribution at steady state after extravascular administration (V_{ss}/F), were calculated.

Results

Human Pharmacokinetics, Excretion, and Metabolism. The mean plasma concentration versus time for LY3202626 in plasma and total radioactivity in both plasma and whole blood after a single 10-mg dose of LY3202626 containing approximately 100 μCi of [^{14}C]LY320262 are shown in Fig. 1. The PK parameters for plasma LY3202626, plasma total radioactivity, and whole blood total radioactivity are presented in Table 1. Radioactivity was quantifiable in plasma up to 96 hours by LSC and up to 504 hours by accelerator mass spectrometry (AMS). The median t_{max} for LY3202626 in plasma was 4.00 hours postdose, with secondary peaks generally observed at approximately 10 hours and again at 24–36 hours postdose. The mean $t_{1/2}$ of plasma LY3202626 was 24.5 hours, with values for individual subjects ranging from 17.0 to 52.2 hours. The last quantifiable time point for LY3202626 in individual subjects ranged from 96 hours postdose (subject 1006) to 336 hours postdose (subject 1002). The median t_{max} values for total radioactivity in plasma and whole blood were 3.50 hours and 4.00 hours postdose, respectively, which is similar to that for plasma LY3202626. Secondary peaks were generally observed for total radioactivity at approximately 10 hours postdose and again at 24–36 hours. The mean $t_{1/2}$ of plasma total radioactivity was 32.5 hours. A $t_{1/2}$ could not be calculated for total radioactivity in whole blood because of the poorly defined terminal phase. The ratios of whole blood to plasma total radioactivity ranged from 0.650 to 0.806 through 10 hours postdose (data not shown). Exposure to LY3202626 accounted for approximately 32% and 42% of total plasma radioactivity based on $AUC_{(0–48)}$ and C_{max}, respectively, indicating the presence of one or more circulating metabolites.

Excretion and Mass Balance in Urine and Feces. The cumulative excretion of total radioactivity up to 504 hours postdose is depicted graphically in Fig. 2. The overall mean (±S.D.) recovery of radioactivity in urine and fecal samples was 75.4% (±4.84%) over the 504-hour study, with recovery in individual subjects ranging from 68.8% to 81.5%. A mean (±S.D.) of 44.2% (±3.70%) of the dose was excreted in urine, and 31.3% (±4.24%) was excreted in feces through the last collection interval. Total radioactivity was excreted slowly, and the majority was recovered in the first 264 hours postdose (approximately 65.6%). The maximum mean amounts of [^{14}C]LY3202626-derived radioactivity were observed in samples collected from 0 to 6 hours postdose for urine (8.50% of the dose) and from 72 to 96 hours postdose in feces (4.72% of the dose). Levels of radioactivity observed in expired air samples were very low (near the limit of quantitation). Therefore, the percentage of dose in expired air was not calculated.

Radioprofiling and Metabolite Identification. Radioprofiling of the 0- to 24-hour AUC plasma pool by AMS showed that parent was the largest peak, accounting for 38.0% of the total radioactivity (Fig. 3; Table 2). Identified metabolites included M1 (the aniline from the amide

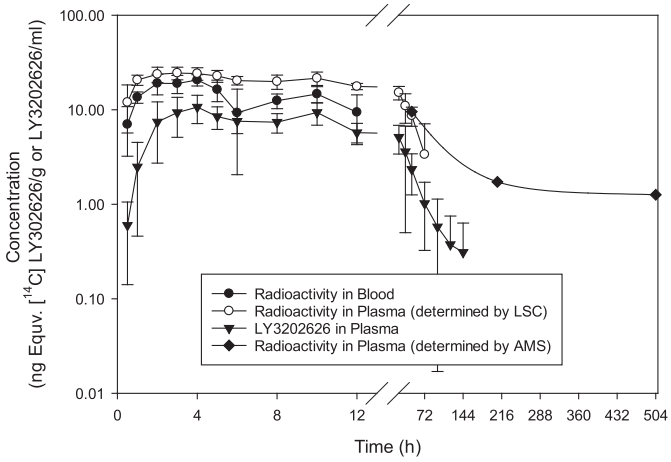

Fig. 1. Mean (±S.D.) concentrations of radioactivity in blood and plasma and mean (±S.D.) concentrations of parent compound (LY3202626) after administration of a single 10-mg (100 μCi) oral dose of [^{14}C]LY3202626 to healthy subjects.

TABLE 1

Summary of pharmacokinetic parameter estimates of LY3202626 in plasma and total radioactivity in plasma and whole blood after oral administration of a single 10-mg dose of [^{14}C]LY3202626

Concentrations of total radioactivity in whole blood were not quantifiable for a sufficient duration to reliably determine $AUC_{(0-\infty)}$. Instead, partial AUCs up to the last common quantifiable time point for all subjects in plasma and whole blood, $AUC_{(0-48)}$, and $AUC_{(0-10)}$, respectively, were used for calculation of ratios of plasma LY3202626 relative to plasma total radioactivity and ratios of whole blood to plasma total radioactivity.

PK Parameters	Geometric Mean (CV%)		
	Plasma LY3202626 (N = 6)	Plasma Total Radioactivity[a] (N = 6)	Whole Blood Total Radioactivity[a] (N = 6)
$AUC_{(0-tlast)}$ (ng·h/ml)	294 (48)	814 (31)	210 (60)
$AUC_{(0-\infty)}$ (ng·h/ml)	298 (47)	1120 (27)	NC
$\%AUC_{(tlast-\infty)}$	1.19 (48)	27.0 (19)	NC
$AUC_{(0-10)}$ (ng·h/ml)	70.0 (36)	207 (14)	146 (17)
$AUC_{(0-48)}$ (ng·h/ml)	227 (37)	711 (15)	NC
C_{max} (ng/ml)	10.7 (32)	25.2 (16)	21.0 (18)
t_{max}[b] (h)	4.00 (2.00–10.00)	3.50 (2.00–5.00)	4.00 (2.00–4.05)
$t_{1/2}$[c] (h)	24.5 (17.0–52.2)	32.5 (25.1–45.4)	NC
CL/F (l/h)	33.6 (47)	NA	NA
V_z/F (l)	1190 (19)	NA	NA
V_{ss}/F (l)	1140 (28)	NA	NA

[a]Data presented as nanograms equivalents per gram, as applicable.
[b]Median (range).
[c]Geometric mean (range).

hydrolysis, LSN3200635), M2 (*O*-desmethyl, LSN3207841), M3 (the carboxylic acid from the amide hydrolysis, LSN3170994), M4 (glycine conjugate of M3), M5 (*N*-acetyl conjugate of M1, LSN3226305), and M16 (M2 − O, M2 reduction, LSN3420637), accounting for 2.27%, 4.41%, 3.86%, 11.90%, <1% and <1% of the total radioactivity, respectively. Because of poor extraction recoveries (<70%), diluted plasma samples were directly injected onto an HPLC column for radioprofiling by AMS. Metabolite identification in plasma was achieved by matching UV traces of synthetic standards spiked in plasma to radioactive peaks. Radioactivity that eluted during column wash (HPLC retention time around 100 minutes) (region A) accounted for 33.5% of the total radioactivity. Pooled plasma samples at 4, 144, and 288 hours were also profiled by AMS. At 4 hours, parent was the largest peak (43.4% of the total radioactivity), and M4 was the most abundant metabolite (10.3% of the total radioactivity). Over time, the relative percentages for M3, M4, and parent decreased, whereas M1, M2, and M16 increased, suggesting rapid elimination of M3, M4, and parent and slow elimination and/or formation of M1, M2, and M16. The relative percent of sample radioactivity for region A increased over time, from 30% at 4 hours to 54% at 288 hours. After extraction of plasma using acetonitrile and methanol (protein precipitation), the percentage of unextracted radioactivity (remaining in protein pellet) matched very well with that in region A in all plasma samples injected directly to AMS (4-, 144-, 288-, and 0- to 24-hour AUC pool). These results suggest that region A might be LY3202626 or metabolites associated with protein-related material(s).

Urine samples collected from 0 to 24, 24 to 312, and 480 to 504 hours were pooled across subjects and profiled. Parent drug, M1, M2, M4, M5, and M21 (having the same molecular ion and similar mass fragments as parent drug) were identified and quantified in urine (Fig. 4; Supplemental Table 1; Table 3). Parent drug accounted for approximately 2% of the dose in the urine samples analyzed. M2 and M4 were the two most abundant urinary metabolites, accounting for 9% and 21% of the dose, respectively, in the urine samples analyzed. In the early collection period (0–24 hours), M4 was the predominant radioactive

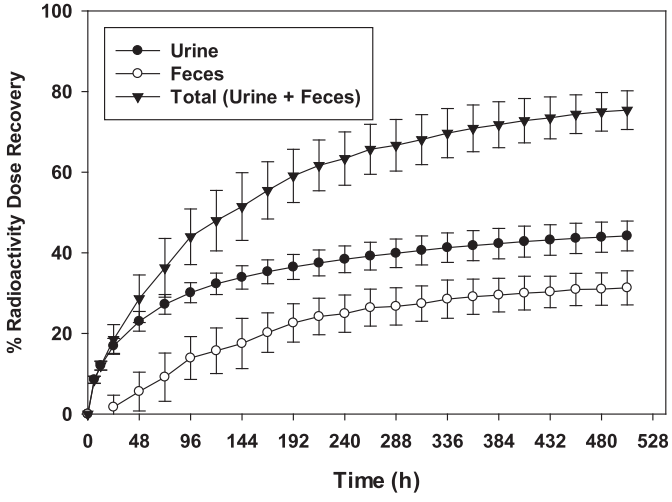

Fig. 2. Mean (+S.D.) cumulative percentage of radioactive dose recovered in urine and feces at specified intervals after administration of a single 10-mg (100 μCi) oral dose of [^{14}C]LY3202626 to healthy subjects.

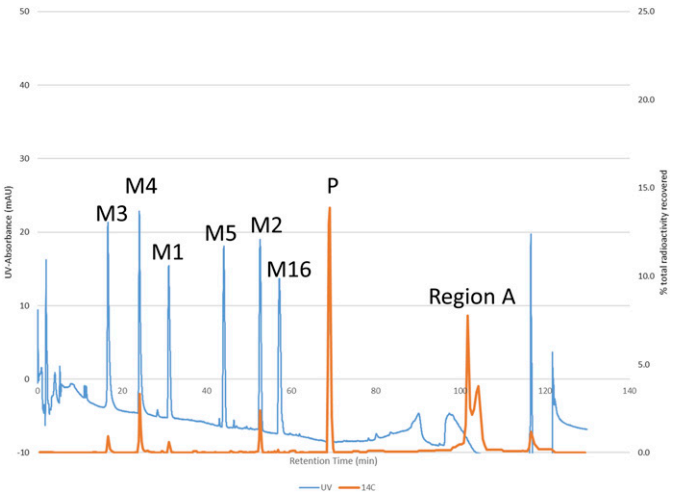

Fig. 3. UV chromatogram (250 nm) generated from injection of diluted plasma spiked with synthetic standards of M1, M2, M3, M4, M5, M16, and P (parent) overlaid against a ^{14}C radiochromatogram based on the AMS detection of fractions and fraction pools collected from direct injection of 0- to 24-hour AUC pool plasma after administration of a single 10-mg (100 μCi) oral dose of [^{14}C]LY3202626 to healthy subjects. Note that UV trace of the parent (P) is obscured by its radioactive trace.

TABLE 2

Percent of sample radioactivity as [^{14}C]LY3202626 or metabolites of [^{14}C]LY3202626 in pooled human plasma samples after a single oral dose of 10 mg of [^{14}C] LY3202626

Peak	Protonated Molecular ion $[M + H]^+$	Proposed Metabolite Identification	Percent of Radioactivity (% of Run)			
			4 hour	144 hour	288 hour	AUC Pool (0–24 hours)
Parent	499	LY3202626	43.4	8.96	1.63	38
M1	363	Amide hydrolysis to the amine (aniline) (LSN3200635)	1.28	17.2	24.3	2.27
M2	485	*O*-desmethyl (LSN3207841)	4.13	11.3	10.3	4.41
M3	155	Amide hydrolysis to the carboxylic acid (LSN3170994)	3.64	<1.0	<1.0	3.86
M4	212	M3 + glycine (LSN3329581)	10.3	1.57	<1.0	11.9
M5	405	*N*-acetyl of M1 (LSN3226305)	<0.5	<1.0	<1.0	<1.0
M16	460	M2 − O (reduction) (LSN3420637)	<1.0	2.1	1.81	<1.0
Region A			30.0	46.9	54.3	33.5
Total			92.76	88.03	92.34	93.94
Total radioactivity recovery			103.0	101.3	103.0	96.7

peak, accounting for 73% of the total radioactivity in sample (Fig. 4). Over time, percentage of radioactivity attributed to M4 decreased (39% in urine samples from 24–312 hours and 0% in urine from 480–504 hours). In contrast, the relative percent radioactivity of M2 compared with total radioactivity increased over time, accounting for 7%, 32%, and 76% of the total radioactivity in urine samples from 0–24, 24–312, and 480–504 hours, respectively. These data suggested relatively rapid excretion for M4 and slow excretion and/or formation for M2. Metabolites M1, M5, and M21, also identified in urine, each accounted for less than 2% of the dose.

Fecal samples collected from 0–24, 24–96, 96–336, and 480–504 hours were pooled across subjects and profiled. Parent drug, M2, M5, M16, and M21 were identified and quantified in feces (Fig. 5; Supplemental Table 1; Table 3). Parent drug accounted for 2% of the dose in the feces analyzed. M2 and M16 were the two most abundant fecal metabolites across all the collection time periods, accounting for approximately 11% and approximately 7% of the dose, respectively, in the feces analyzed. M5 and M21 individually accounted for less than 2% of the dose in the feces analyzed. In the feces from 480–504 hours, M2 and M16 were the only radioactive peaks observed.

In Vitro Incubations. A small percentage of plasma radioactivity (region A) could not be extracted, and the relative percentage of this unextractable radioactivity increased over the time of plasma collection (Table 2). The percentage of unextracted radioactivity (remaining in protein pellet) matched very well with that in region A in various plasma samples, suggesting that region A might be LY3202626 or metabolites associated with protein-related material(s). It is known that some sulfur-containing drugs may form reactive sulfenic acid species that in turn can react with nucleophilic moieties of proteins (Mansuy and Dansette, 2011). Dimedone has been quite successfully used as a trapping agent to capture sulfenic acid species formed by metabolic activation in vitro (Gupta and Carroll, 2016)(Gupta et al., 2016)(Gupta and Carroll, 2016; Gupta et al., 2016). To assess the possible formation of a reactive sulfenic acid metabolite, LY3202626 was incubated in human liver microsomes in the presence of dimedone and in the presence and absence of NADPH. LY3202626-dimedone adducts were observed in the presence of NADPH but not in the absence of NADPH (Fig. 6).

To investigate potential for reduction of M2 to M16 in the gut, an incubation of M2 with human fecal microflora under anaerobic atmosphere was conducted. The results showed the reduction of M2 to M16 in human fecal microflora under anaerobic atmosphere, but no such reduction was observed in medium control or with heat-deactivated fecal microflora (Fig. 7). The permeability of M2 and M16 was also evaluated by studying transport across MDCK-MDR1 monolayers. Results showed M2 as a highly efficient P-glycoprotein (P-gp) substrate with very slow passive permeability, whereas M16 is a moderate P-gp substrate with very fast passive permeability and fast permeability even against the active efflux pump (160 nm/s) (Table 4).

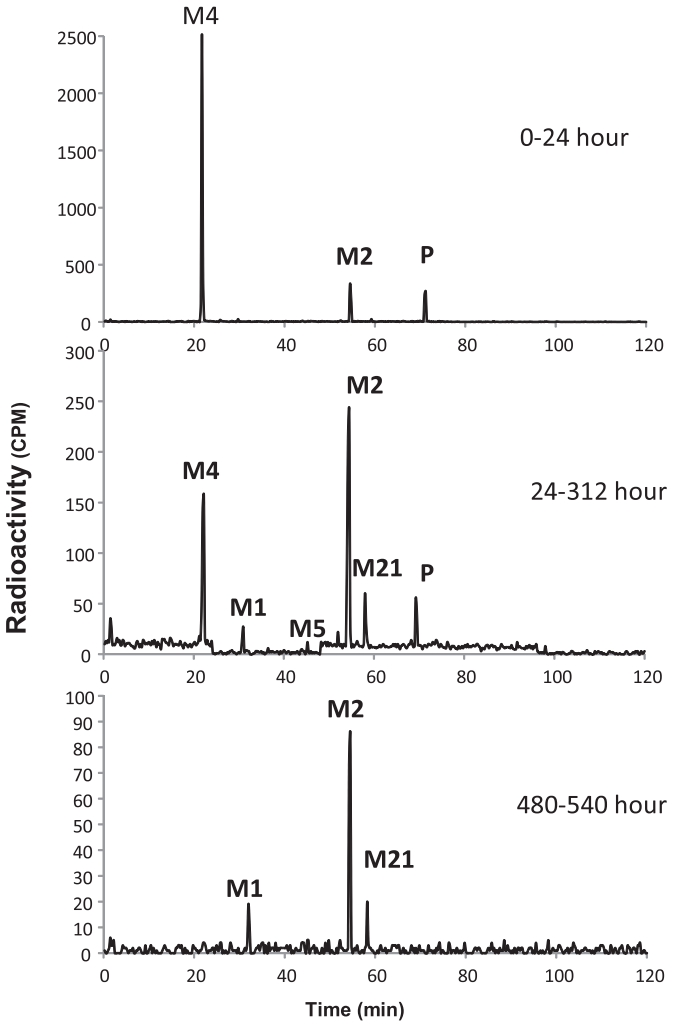

Fig. 4. Reconstructed radioprofiles of urine after administration of a single 10-mg (100 μCi) oral dose of [^{14}C]LY3202626 to healthy subjects. P, parent,

TABLE 3

Percent dose of LY3202626 and its metabolites excreted in urine and feces from healthy human subjects after a single oral dose of 10 mg of [^{14}C]LY3202626 from 0 to 508 hours

Peak	Protonated Molecular ion $[M + H]^+$	Proposed Metabolite Identification	Percent of Dose		
			Urine	Feces	Total
Parent	499	LY3202626	2.25	2.02	4.27
M1	363	Amide hydrolysis to the amine (aniline) (LSN3200635)	1.21	ND	1.21
M2	485	*O*-desmethyl (LSN3207841)	8.88	10.75	19.63
M4	212	M3 + glycine (LSN3329581)	21.27	ND	21.27
M5	405	*N*-acetyl of M1 (LSN3226305)	0.18	1.32	1.5
M16	460	M2 − O (reduction) (LSN3420637)	ND	6.94	6.94
M21	499	Same mass as parent	1.34	1.55	2.89
Total % identified			35.15	22.57	57.72
Total % dose in the sample analyzed			40.99	28.81	69.8

To investigate the potential for the oxidation of M16 to M2, M16 (LSN3420637) was incubated in rat, dog, monkey, and human hepatocytes. The results showed the formation of M2 in rat, monkey, and human hepatocytes but not in dog hepatocytes. M2 formation from M16 was inhibited by hydralazine (an aldehyde oxidase inhibitor; Sun et al., 2011; Strelevitz et al., 2012) but not by ABT (a pan–cytochrome P450 inhibitor, Ortiz de Montellano and Mathews, 1981; Johnson et al., 1985; Williams et al., 2003) (Supplemental Table 2). M16 incubations in hepatocytes also showed the formation of another hydroxy metabolite M1 in all the species, which was not inhibited by ABT or hydralazine. Figure 8 shows the extracted ion chromatograms from these incubations in human hepatocytes. To confirm the position of the oxidation of M2 generated from M16 in vitro, M16 was incubated in human liver cytosol, and M2 was isolated from the incubation and analyzed by NMR. The NMR result confirmed that M2 generated from M16 is LSN3420637 (data not shown). It should be noted that the concentration of hydralazine used in these incubations was high (i.e., 200 μM), which could possibly inhibit some of the cytochrome P450 enzymes (Yang et al., 2019). However, lack of the formation of M2 by dog hepatocytes, no inhibition of the formation of M2 in the presence of ABT, and the isolation of M2 using human cytosols provide additional support that the M2 is formed by AO and not cytochrome P450 enzymes.

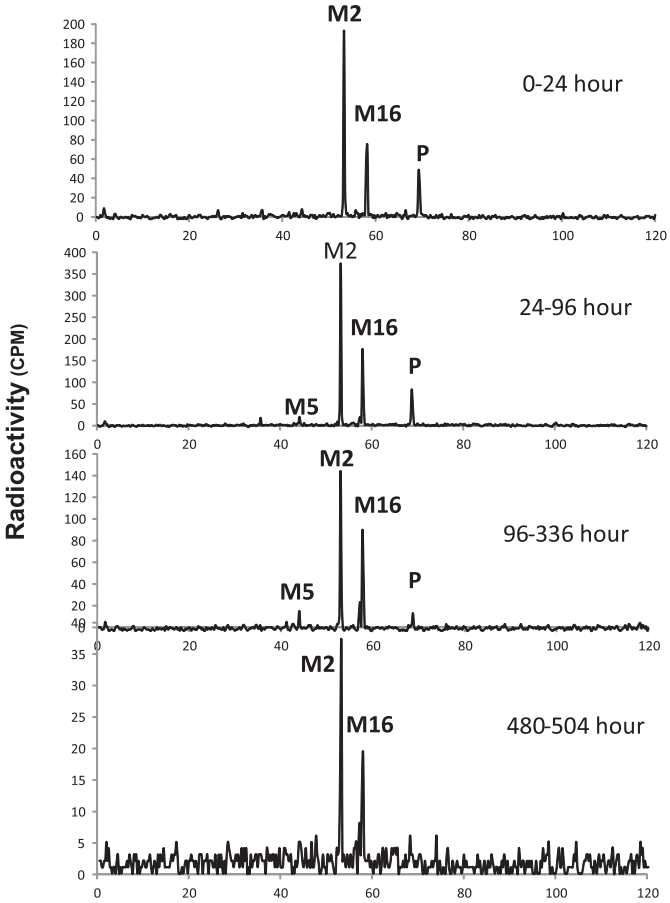

Fig. 5. Reconstructed radioprofiles of feces after administration of a single 10-mg (100 μCi) oral dose of [^{14}C]LY3202626 to healthy subjects. P, parent.

Discussion

In this study, [^{14}C]LY3202626 was administered orally at a pharmacologically relevant dose of 10 mg (100 μCi) to six healthy male volunteers (https://clinicaltrials.gov/ct2/show/NCT02555449). After collection of excreta for up to the maximum of 21 days, only

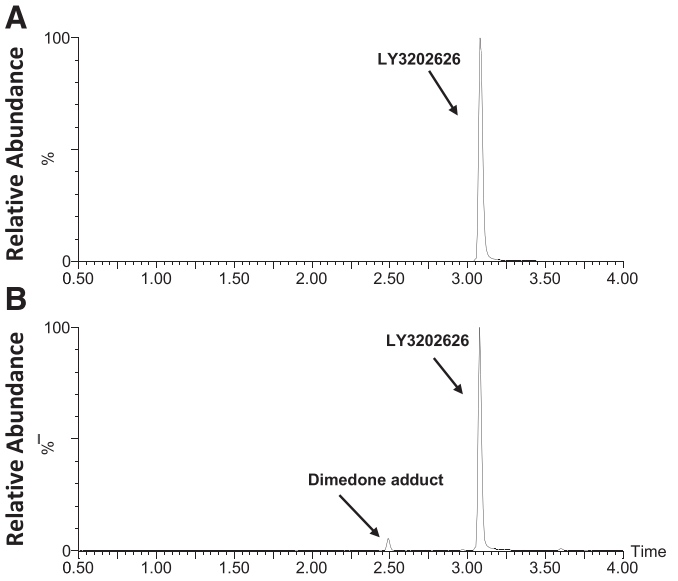

Fig. 6. (A) Extracted ion chromatograms of LY3202626 and its dimedone adduct after incubation of LY3202626 in human liver microsomes in the absence (A) and presence of NADPH (B). (B) The proposed metabolic pathway for the formation of LY3202626-dimedone adduct after incubation of LY32026 in human liver microsome incubations in the presence of NADPH and dimedone.

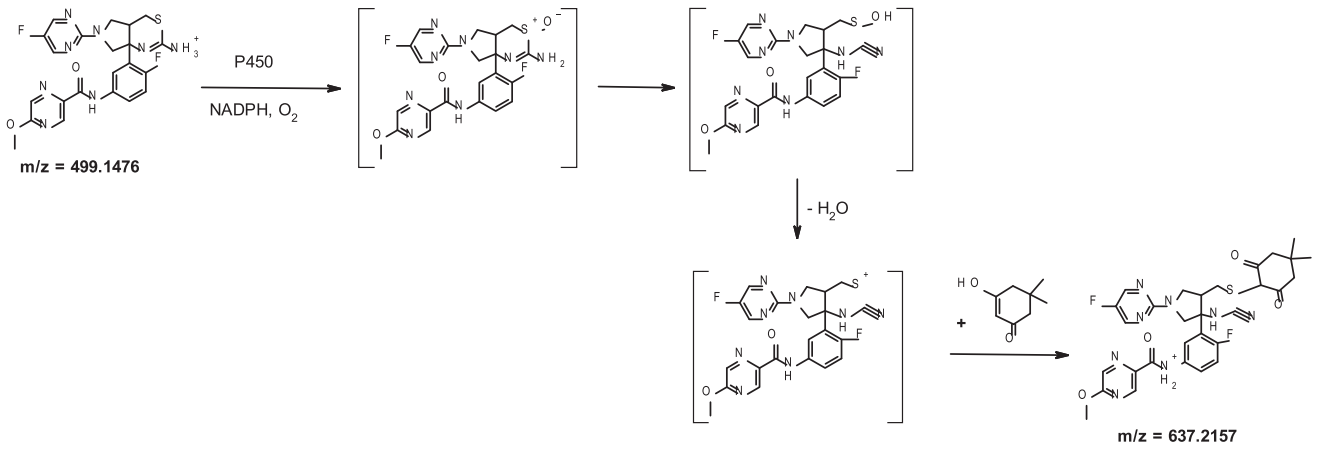

Fig. 6. Continued.

74.5% (31.4% urine and 44% feces) of the dose was recovered in urine and feces, with no appreciable amount of radioactivity obtained in expired air.

Although there is no formal cutoff for "acceptable" recovery in a human absorption, distribution, metabolism, and excretion (ADME) study, the overall recovery from this study falls well within the data reported by Roffey et al. (2007). The overall recovery from this study was sufficient to meet the objectives of the study, which included understanding the major clearance pathways as well as identification of the major metabolites. The pharmacokinetics of LY3202626 and total radioactivity also showed unusual characteristics, with secondary peaks observed in the PK profiles of LY3202626 (plasma) and total radioactivity (blood and plasma) following the C_{max} peaks at 4.0, 3.5, and 4.0 hours, respectively. The secondary peaks for LY3202626 and for total radioactivity appeared between 10 and 36 hours postdose. A metabolite (M21, Fig. 9) whose structure could not be determined has the same molecular and product ion as parent, suggesting it could be a phase II conjugate that is unstable when ionized in the mass spectrometer, undergoing source-induced fragmentation. It is possible that such a labile phase II conjugate could be hydrolyzed in the intestine, followed by reabsorption, leading to the secondary peaks observed for LY3202626 and total radioactivity. Exposure to LY3202626 accounted for approximately 32% and 42% of total plasma radioactivity based on $AUC_{(0-48)}$ and C_{max}, respectively, indicating the presence of one or more circulating metabolites. Overall, parent drug, M1, M2, M3, and M4 were the predominant circulating components in plasma, and M2 and M4 were the predominant excretory metabolites. Parent drug and M4 were the only components in plasma that accounted for >10% of radioactivity in the $AUC_{(0-24)}$. Over time, the relative percentages for M3, M4, and parent decreased in plasma, whereas M1, M2, and M16 increased, suggesting rapid elimination of M3, M4, and parent and slower elimination and/or formation of M1, M2, and M16.

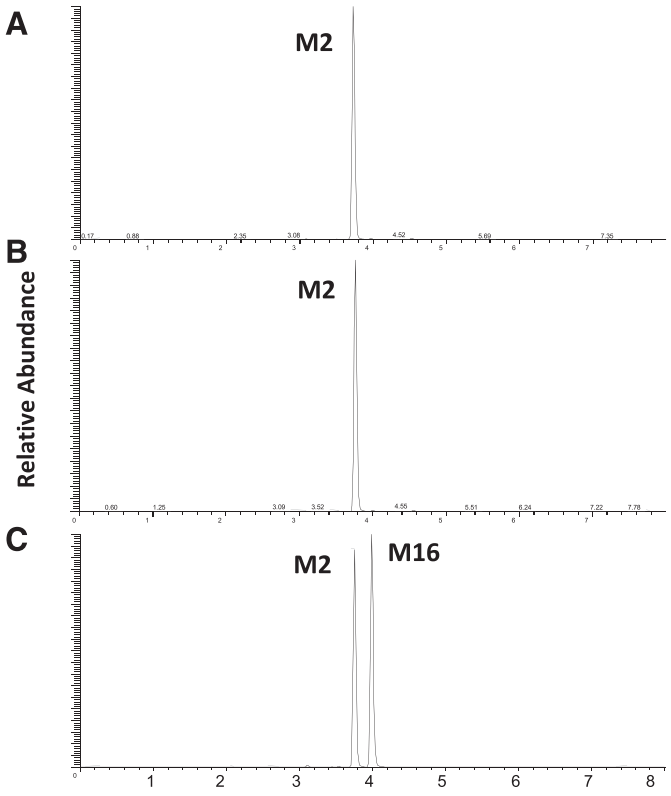

Fig. 7. Extracted ion chromatograms of M2 (LSN3207841) and incubations under anaerobic condition for 168 hours with brain heart infusion medium (A), with deactivated human fecal microflora (B) and non-deactivated human fecal microflora (C).

LY3202626 was well absorbed and extensively metabolized in healthy subjects after a single oral dose of 10 mg of [^{14}C]LY3202626, with only 4% of dose excreted as parent drug in urine and feces. In urine, parent drug accounted for approximately 2% of the dose, and metabolites M2 and M4 were the two most abundant urinary metabolites, accounting for 9% and 21% of the dose, respectively. In feces, parent drug accounted for 2% of the dose, and metabolite M2 and M16, the two most abundant fecal metabolites, accounting for approximately 11% and 7% of the dose, respectively. Overall, the data from the study demonstrates that metabolism is the major route of clearance for LY3202626, and metabolism of LY3202626 occurs primarily through *O*-demethylation (M2) and amide hydrolysis (M1, M3, M4, and M5). Figure 9 shows proposed metabolism pathways of LY3202626 in humans.

As previously discussed, the mass balance excretion results from this study appeared less than optimal and were somewhat unanticipated. In preclinical ^{14}C ADME studies conducted prior to the human ADME study, the recovery of radioactive dose was almost 100% by 168 hours in rats and >90% by 192 hours in dogs (Supplemental Fig. 1). Furthermore, radioactivity was eliminated rapidly, with approximately 97% of the total radioactive dose

TABLE 4

Permeability in MDCK-MDR1 monolayers for LSN3207841(M2) and LSN3420637 (M16) and LSN3182170 (HCl salt of LY3202626, parent)

Compound		rD0, μM	Pe ± S.D. × 10^{-6} cm/s	% Cell ± S.D.	% Recovery	Pe $_{BL/AP}$	Pe $_{c/l}$	P-gp	P-gp Inhibition %		Comments
									5 μM	25 μM	
M2				P-gp inhibited				Yes	0	0	Very slow Pe, very low % cell, inhibition unlikely
	A-B	3.5	1.1 ± 0.25	0.34 ± 0.00	102 ± 0.56	0.71	29				
	B-A	3.3	0.80 ± 0.00	0.31 ± 0.00	100 ± 5.1						
				P-gp active							
	A-B	3.3	0.57 ± 0.05	0.30 ± 0.02	100 ± 1.4	21					
	B-A	3.4	12 ± 0.26	0.27 ± 0.02	89 ± 3.6						
M16				P-gp inhibited				Yes	1	21	Fast Pe, moderate % cell, inhibition unlikely
	A-B	3.5	53 ± 0.14	20 ± 0.18	154 ± 0.40	0.99	6.1				
	B-A	2.8	53 ± 0.04	19 ± 0.73	130 ± 3.9						
				P-gp active							
	A-B	2.6	16 ± 2.1	11 ± 0.09	115 ± 5.7	6.0					
	B-A	2.6	97 ± 0.62	7.9 ± 0.42	125 ± 4.1						
Parent				P-gp inhibited				No	6	25	Fast Pe, high partitioning, inhibition unlikely
	A-B	2.1	19 ± 2.3	50 ± 0.53	92 ± 8.6	1.2	1.5				
	B-A	2.4	21 ± 0.02	28 ± 0.00	97 ± 5.5						
				P-gp active							
	A-B	2.8	15 ± 0.13	49 ± 1.6	88 ± 0.25	1.8					
	B-A	2.7	27 ± 1.1	27 ± 5.4	94 ± 1.4						

rD0 is the measured concentration of recovered donor solution at t = 60 min. Pe is the apparent permeability coefficient (n = 2) with 60-min time interval: AB, BA>15, fast; AB, BA is 2–15, moderate; AB, BA is 1–2, slow; AB, BA is <1, very slow. % Cell is the amount extracted from cell with methanol relative to recovered mass: <1%, very low; 1%–5%, low; 6%–20%, moderate; 21%–89%, high; ≥90%, very high (invalidates Pe values because compound prefers lipid environment, assay artifact). %Recovery is the mass of D60 + cell60 + R60/D0 (measured concentration of donor solution at t = 0) × 100. If >100%, then D0 is underestimated. Pe $_{BL/AP}$ is the ratio of Pe values in B-to-A and A-to-B directions; >3.0 + active efflux; Pe $_{C/I}$ is the net efflux ratio = inhibited BA/AB and control BA/AB ratio. P-gp Yes (Y), No (*N*), or Unknown (U): if ≥3, Y; <3, *N*; if % Cell > 90, U. P-gp inhibition, two concentrations (5 and 25 μM) tested for calcein AM uptake assay in MDCK-MDR1 cells; % inhibition vs. LSN335984 (EC_{50} = 0.15–0.3 μM), pending at 5 μM: 0–20, inhibition unlikely, 21–50, partial inhibition possible, >51%, partial inhibition likely.

eliminated in the first 48 hours postdose after a single oral administration in rat and approximately 84% of the dose eliminated in the first 72 hours postdose after a single oral administration in dog. Particularly slow excretion of radioactivity in both urine and feces in humans, as well as slow clearance of some of the metabolites (M1, M2, and M16) from plasma, was puzzling.

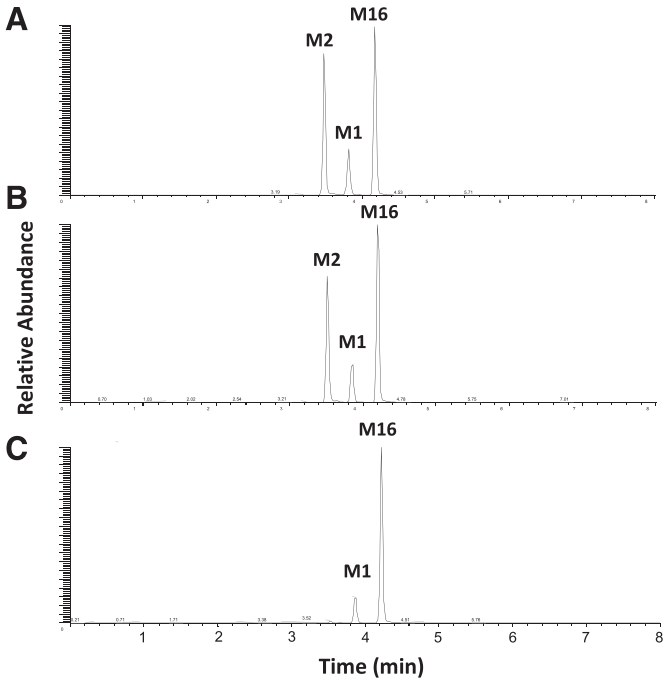

Fig. 8. Extracted ion chromatograms of M16 (LSN3420637) incubations in human hepatocytes for 4 hours in the absence of any inhibitor (A), in the presence of ABT (B), and in the presence of hydralazine (C).

Furthermore, a percentage of plasma radioactivity could not be extracted (region A), and this unextractable region represented a greater percentage of radioactivity in plasma samples at later time points. In contrast, the percentage of plasma radioactivity recovery was almost complete in rat and dog (86%–94% for rat and 95%–100% for dog; Supplemental Table 3, A and B). The amount of radioactivity found in the human plasma protein pellet (when resuspended using acetonitrile and methanol), matched the amount of radioactivity represented by region A at various time points after direct injection of diluted plasma, and these data suggest that region A might be LY3202626 and/or metabolites associated with protein-related material(s). Sulfur-containing drugs are known to possibly form reactive sulfenic acid species that in turn may react with nucleophilic (sulfhydryl) moieties of proteins (Mansuy and Dansette, 2011). The observation of a LY3202626-dimedone adduct formed in human liver microsome incubations containing NADPH and dimedone (Fig. 6) supports the hypothesis that the unextractable portion of radioactivity in plasma could be due to one or more adducts formed by a sulfenic acid metabolic intermediate of LY3202626 reacting with plasma protein to form a covalent adduct.

Metabolite M4 was the predominant radioactive peak in the 0- to 24-hour urine sample, but it was not quantifiable in the 480- to 504-hour sample (Fig. 4). In contrast, the relative percent radioactivity of M2 increased over time. In feces, M2 and M16 were the two most abundant fecal metabolites across all the collection time periods (Fig. 5). In fact, M2 and M16 were the only radioactive peaks observed in the 480- to 504-hour feces. Based upon the slow excretion of radioactivity, the presence of M2 as the most prominent metabolite peak at later time points in urine, and the presence of M2 and M16 as the two most abundant fecal metabolites at all the collection time periods, it was hypothesized that the slow excretion of radioactivity in excreta could be due to reduction/oxidation cycling between M2 and M16. To investigate this possibility,

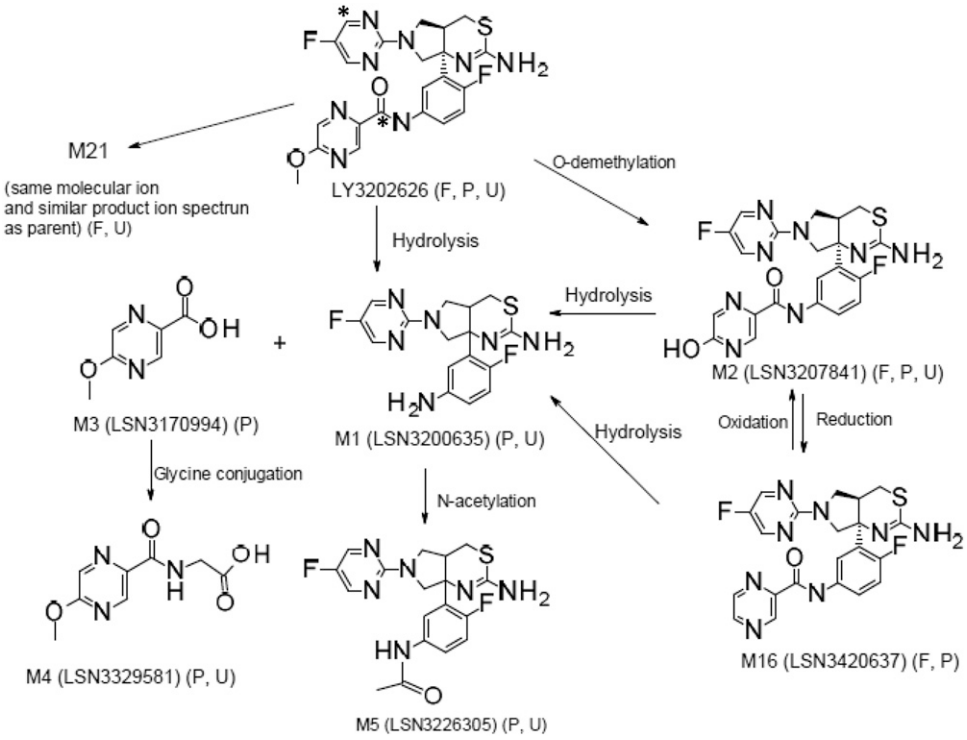

Fig. 9. The proposed metabolic scheme for LY3202626 after a single 10-mg oral dose of [^{14}C]LY3202626 to healthy humans. This test article is dual radiolabeled, and the dosing included 1:1 mix of both labeled compounds; * signifies the positions of the radiolabel. F, P, and U indicate presence in feces, plasma and urine, respectively.

several in vitro experiments were conducted. Formation of M2 from M16 in rat, monkey, and human hepatocytes but not in dog hepatocytes and inhibition of the formation of M2 from M16 in the presence of hydralazine but not in the presence of ABT suggested that metabolism of M16 to M2 is mediated by AO. To confirm that M2 was formed via AO from M16, metabolite M16 was incubated in human cytosol, and M2 was isolated and purified. The NMR spectra obtained from the cytosol incubation matched M2 (data not shown). Incubation of metabolite M2 with human feces under an anaerobic atmosphere showed that M2 is reduced to M16 by gut microflora. In addition, an in vitro permeability assessment showed that M2 is a highly efficient P-gp substrate with very slow passive permeability. In contrast, M16 was found to be a moderate P-gp substrate with very fast passive permeability (Table 4). Based upon these results, we propose that LY3202626 is first converted to M2 by cytochrome P450 demethylation, which gets excreted into intestine, where its very low permeability and P-gp substrate recognition prevent reabsorption. Metabolite M2 is then anaerobically reduced to M16 by gut microflora, and the resulting highly permeable M16 is reabsorbed. After reabsorption, metabolite M16 is oxidized back to M2 in the liver by AO or hydrolyzed to M1, as illustrated in Fig. 10. Such enterohepatic recirculation might contribute to extended retention of M1, M2, and M16. The reduction/oxidation reactions form a complete enterohepatic cycling process. The lack of an extended excretion profile of radioactivity due to M2/M16 enterohepatic recirculation in preclinical species administered [^{14}C]LY3202626 could be due to the minimal formation of M2 in rat and inherited lack of AO activity in dog (Supplemental Table 4). Li et al. (2012) reported a similar reduction and oxidation of BILR 355 (an inhibitor of the human immunodeficiency virus) by gut bacteria and AO, respectively. In that particular study, ritonavir was used to inhibit the CYP3A-mediated metabolism of BILR 355 and to increase the clinical exposure of BILR 355. However, the inhibition not only increased the levels of BILR 355, but a metabolite (BILR 516) that was not detected previously in humans dosed with BILR 355 alone was found. Subsequent in vitro studies revealed that a metabolic switching of BILR 355 occurs in the presence of ritonavir. BILR 355 is

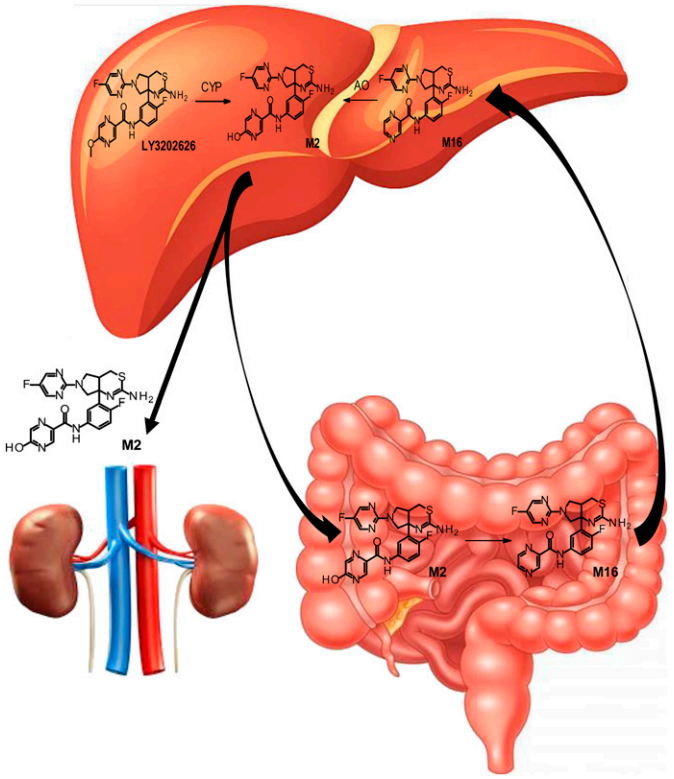

Fig. 10. Hypothesis illustrating enterohepatic recirculation of radioactive material and possible cause of slow excretion of radioactivity, involving microbial reduction of metabolite M2 to M16 in the gut and reabsorption of M16, followed by hepatic oxidation of M16 back to M2.

reduced to an intermediate, BILR 402, by gut bacteria, and the reduced metabolite (BILR 402) is then oxidized by aldehyde oxidase to form BILR 516, the disproportionate human metabolite. Ross et al. (1988) similarly reported that 5-(4-acetamidopheyl)pyrazine-2(1H)-one, containing a pyrazinone moiety, a structure similar to the hydroxy pyrazine in M2, undergoes reduction of the pyrazinone to the corresponding pyrazine metabolite by microflora in gut. The authors speculated that the pyrazine metabolite might be reabsorbed from gut and subsequently oxidized in liver to an *N*-oxide.

In conclusion, after administration of a single 10-mg oral dose of [^{14}C]LY3202626 to humans, overall recovery of radioactivity even after 3 weeks of collection was only 75%, which falls well within the data reported by Roffey et al. (2007). The overall recovery from this study was sufficient to meet the objectives of the study, which included understanding the major clearance pathways as well as identification of the major metabolites. Several in vitro experiments carried out with LY3202626 provided strong support for the proposed mechanisms leading to the long retention of radioactivity in circulation and excreta, as illustrated in Fig. 10. Similar observations of enterohepatic recirculation have also been made previously (Ross et al., 1988; Li et al., 2012). Another important observation from the study was that a portion of plasma radioactivity was unextractable. Observation of a dimedone adduct after in vitro incubation of LY322626 with liver microsome and dimedone suggests that the unextracted plasma radioactivity could be due to formation of plasma protein adducts by reactive sulfenic acid metabolite intermediates of LY3202626. Considering a proposed therapeutic dose of 10 mg, the body burden due to formation of such a reactive intermediate would have been expected to be low (Lammert et al., 2008; (Stepan et al., 2011)Stepan et la., 2011). However, as further development of this compound was halted, any impact of such a reactive intermediate in humans will be unknown.

Acknowledgments

The authors would like to acknowledge Jeffrey Alberts and Geri Sawada for performing dimedone trapping assays and permeability assays, respectively.

Authorship Contributions

Participated in research design: Katyayan, Yi, Monk, Cassidy.
Conducted experiments: Yi.
Contributed new reagents or analytic tools: Katyayan, Yi, Cassidy.
Performed data analysis: Katyayan, Yi, Cassidy.
Wrote or contributed to the writing of the manuscript: Katyayan, Monk, Cassidy.

References

FDA (2020a) *Guidance for Industry: Safety Testing of Drug Metabolites, Version 2, US Department of Health and Human Services FDA*, Center for Drug Evaluation and Research, Silver Spring, MD.
FDA (2020b) *In Vitro Drug Interaction Studies — Cytochrome P450 Enzyme- and Transporter-Mediated Drug Interactions Guidance for Industry, US Department of Health and Human Services FDA*, Center for Drug Evaluation and Research, Silver Spring, MD.
Gupta V and Carroll KS (2016) Profiling the reactivity of cyclic *C*-nucleophiles towards electrophilic sulfur in cysteine sulfenic acid. *Chem Sci (Camb)* **7**:400–415.
Gupta V, Paritala H, and Carroll KS (2016) Reactivity, selectivity and stability in sulfenic acid detection: a comparative study of nucleophilic and electrophilic probes. *Bioconjug Chem* **27**: 1411–1418.
Hamilton RA, Garnett WR, and Kline BJ (1981) Determination of mean valproic acid serum level by assay of a single pooled sample. *Clin Pharmacol Ther* **29**:408–413.
Hop CECA, Wang Z, Chen Q, and Kwei G (1998) Plasma-pooling methods to increase throughput for in vivo pharmacokinetic screening. *J Pharm Sci* **87**:901–903.
Johnson C, Stubley-Beedham C, and Stell JG (1985) Hydralazine: a potent inhibitor of aldehyde oxidase activity in vitro and in vivo. *Biochem Pharmacol* **34**:4251–4256.
Lammert C, Einarsson S, Saha C, Niklasson A, Bjornsson E, and Chalasani N (2008) Relationship between daily dose of oral medications and idiosyncratic drug-induced liver injury: search for signals. *Hepatology* **47**:2003–2009.
Li Y, Xu J, Lai WG, Whitcher-Johnstone A, and Tweedie DJ (2012) Metabolic switching of BILR 355 in the presence of ritonavir. II. Uncovering novel contributions by gut bacteria and aldehyde oxidase. *Drug Metab Dispos* **40**:1130–1137.
Mansuy D and Dansette PM (2011) Sulfenic acids as reactive intermediates in xenobiotic metabolism. *Arch Biochem Biophys* **507**:174–185.
Ortiz de Montellano PR and Mathews JM (1981) Autocatalytic alkylation of the cytochrome P-450 prosthetic haem group by 1-aminobenzotriazole. Isolation of an NN-bridged benzyne-protoporphyrin IX adduct. *Biochem J* **195**:761–764.
Penner N, Klunk LJ, and Prakash C (2009) Human radiolabeled mass balance studies: objectives, utilities and limitations. *Biopharm Drug Dispos* **30**:185–203.
Roffey SJ, Obach RS, Gedge JI, and Smith DA (2007) What is the objective of the mass balance study? A retrospective analysis of data in animal and human excretion studies employing radiolabeled drugs. *Drug Metab Rev* **39**:17–43.
Ross DA, Osborne PM, Pue MA, Blake TJ, Chenery RJ, and Metcalf R (1988) The metabolism of 5-(4-acetamidophenyl)pyrazin-2(1H)-one in rat, dog and cynomolgus monkey. *Xenobiotica* **18**: 1373–1387.
Stepan AF, Walker DP, Bauman J, Price DA, Baillie TA, Kalgutkar AS, and Aleo MD (2011) Structural alert/reactive metabolite concept as applied in medicinal chemistry to mitigate the risk of idiosyncratic drug toxicity: a perspective based on the critical examination of trends in the top 200 drugs marketed in the United States. *Chem Res Toxicol* **24**:1345–1410.
Strelevitz TJ, Orozco CC, and Obach RS (2012) Hydralazine as a selective probe inactivator of aldehyde oxidase in human hepatocytes: estimation of the contribution of aldehyde oxidase to metabolic clearance. *Drug Metab Dispos* **40**:1441–1448.
Sun Q, Harper TW, Dierks EA, Zhang L, Chang S, Rodrigues AD, and Marathe P (2011) 1-Aminobenzotriazole, a known cytochrome P450 inhibitor, is a substrate and inhibitor of N-acetyltransferase. *Drug Metab Dispos* **39**:1674–1679.
Williams JA, Hurst SI, Bauman J, Jones BC, Hyland R, Gibbs JP, Obach RS, and Ball SE (2003) Reaction phenotyping in drug discovery: moving forward with confidence? *Curr Drug Metab* **4**: 527–534.
Yang X, Johnson N, and Di L (2019) Evaluation of cytochrome P450 selectivity for hydralazine as an aldehyde oxidase inhibitor for reaction phenotyping. *J Pharm Sci* **108**: 1627–1630.

Address correspondence to: Dr. Kishore K. Katyayan, Eli Lilly and Company, Lilly Corporate Center, Indianapolis, IN 46285. E-mail: kishore.katyayan@lilly.com